Polymorphism of Cocrystals: The Promiscuous Behavior of Agomelatine

Rafel Prohens,[*,†] Rafael Barbas,[†] Anna Portell,[†] Mercè Font-Bardia,[‡] Xavier Alcobé,[‡] and Cristina Puigjaner[*,†]

[†]Unitat de Polimorfisme i Calorimetria and [‡]Unitat de Difracció de Raigs X, Centres Científics i Tecnològics, Universitat de Barcelona, Baldiri Reixac 10, 08028 Barcelona, Spain

ABSTRACT:

It has been traditionally suggested that polymorphism of cocrystals is a phenomenon seen less frequently than in monocomponent crystals. However, since the research on cocrystals has recently experienced a big growth, the number of solved structures of polymorphic cocrystals in the Cambridge Structural Database has increased, which can help to understand better whether a lower impact of this phenomenon exists or not in multicomponent crystals. In this paper we describe the cocrystal landscape of agomelatine, a particularly promiscuous drug able to cocrystallize with up to nine different coformers. Interestingly, two of those coformers have produced polymorphic cocrystals during the screening, which converts agomelatine into a new example that questions the traditional belief of the lesser impact of polymorphism in cocrystals and highlights the importance of polymorphism studies in cocrystal screening. Our work is completed with the determination of the crystal structures of the new forms from combined single crystal/ laboratory X-ray powder diffraction data.

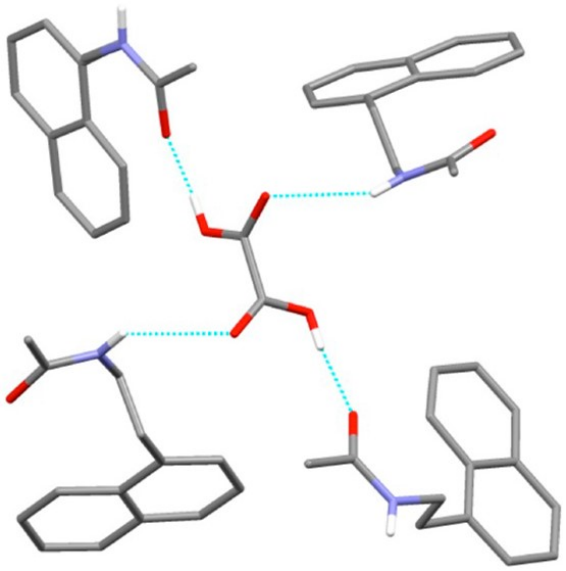

1. INTRODUCTION

Polymorphism of active principle ingredients (API) is almost omnipresent.1 In fact, published data from experimental screens suggest that 80−90% of organic compounds can exist in multiple crystalline forms (polymorphs and solvates) and half of the organic compounds can be polymorphic.2 In recent years, the number of new crystal forms for a drug has been much increased since the erruption of cocrystals in the solid state arena, which offers many opportunities to modify their bulk properties, such as solubility, bioavailability and stability. According to Butterhof et al.,3 the number of characterized polymorphs and cocrystals in 2012 was 2050 and 3650, respectively. In 2010 Zaworotko et al.4 analyzed 38 polymorphic cocrystals, revealing that in 35 polymorphic pairs polymorphism is the result of conformational flexibility and/or structural changes in the packing.

Moreover, an exhaustive search in the literature by Aitipamula et al. in 20135 revealed a total of 110 neutral polymorphic cocrystals. The lower propensity of cocrystals to exhibit polymorphism has been then called into question, and probably a bigger corpus of crystallographic data will be required before the question can be reliably answered.6 Since multicomponent crystals are increasingly relevant in the pharmaceutical industry with cocrystal screenings being routinely performed, a better understanding of polymorphism of cocrystals is a real need. In this paper we intend to contribute new data in order to enrich this relevant debate. Agomelatine (N-[2-(7-methoxynaphthalen-1-yl)ethyl]-acetamide) (Figure 1), under the trade name of Valdoxan or Melitor, is an effective drug for the treatment of major depressive disorders7 first produced by Servier pharmaceutical company in 2009. It has been reported to exist as six polymorphic modifications (Forms I−VI). The crystal structures of Forms I, II, and III have been determined8,9 by single and powder X-ray diffraction, and cocrystals with acetic acid, ethylene glycol, urea, glycolic acid, isonicotinamide, and methyl 4-hydroxybenzoate have been synthesized and structurally characterized.9,10

The pharmaceutical relevance of this compound together with the existence of a big number of different multicomponent crystal modifications prompted us to study its cocrystal promiscuity in relation with the presence of polymorphism. In this contribution, we take a step forward in the investigation of the solid-state landscape of agomelatine by presenting new polymorphic cocrystals with acetic acid and hydroquinone, together with cocrystals with pyruvic acid and oxalic acid.

.

2. MATERIALS AND METHODS

2.1. Synthesis of the New Crystal Forms. 2.1.1. Hydroquinone Cocrystal Ago-HQ Form I. 100 milligrams (0.41 mmol) of agomelatine and 45 mg (0.41 mmol) of hydroquinone were dissolved in 0.1 mL of acetone or ethyl acetate. Crystals suitable for single crystal X-ray diffraction (SCXRD) were obtained after evaporation of the solvent at room temperature after 2 days (mp 81 °C).

2.1.2. Hydroquinone Cocrystal Ago-HQ Form II. Twenty milligrams (0.08 mmol) of agomelatine and 10 mg (0.09 mmol) of hydroquinone were grinded in a ball mill with the addition of one drop of acetonitrile during 30 min at 30 Hz (mp 93 °C).

2.1.3. Oxalic Acid Cocrystal Ago-OA Form I. Twenty milligrams (0.08 mmol) of agomelatine and 7 mg (0.08 mmol) of oxalic acid were dissolved in 50 μL of isopropanol at 40 °C, and the solution was cooled to room temperature in a closed vial. Crystals suitable for SCXRD were obtained after 1 day (mp 87°C).

2.1.4. Acetic Acid Cocrystal Ago-AA Form II. 80 milligrams (0.33 mmol) of agomelatine were dissolved in 50 μL of acetic acid at 45 °C, and the solution was cooled to room temperature in a closed vial. Crystals suitable for SCXRD were obtained after 20 days (mp 65 °C).

2.1.5. Pyruvic Acid Cocrystal Ago-PA. 200 milligrams (0.82 mmol) of agomelatine were dissolved in 0.5 mL of pyruvic acid at 50 °C. The solution was cooled to 5 °C in a closed vial, and crystals suitable for SCXRD were obtained after 5 days (mp 69 °C).

2.2. Methods. 2.2.1. Powder X-ray Diffraction (PXRD). Powder Xray diffraction patterns were obtained on a PANalytical X'Pert PRO MPD diffractometer in transmission configuration using Cu Kα1 + 2 radiation (λ = 1.5418 Å) with a focalizing elliptic mirror and a PIXcel detector working at a maximum detector's active length of 3.347°. Capillary geometry has been used with samples placed in glass capillaries (Lindemman) of 0.5 mm of diameter measuring from 2 to 60° in 2θ, with a step size of 0.026° and a total measuring time of 30 min. Flat geometry has been used for routine samples sandwiched between low absorbing films (polyester of 3.6 μm of thickness) measuring 2theta/theta scans from 2 to 40° in 2θ with a step size of 0.026° and a measuring time of 76 s per step. The PXRD pattern of hydroquinone cocrystal was obtained using synchrotron radiation at ALBA's beamline BL04-MSPD using Mythen detector. The wavelength, 0.6196 Å, was selected with a double-crystal Si (111) monochromator and determined from a Si640d NIST standard (a = 5.43123 Å) measurement. The diffractometer is equipped with a socalled MYTHEN detector system especially suited for time-resolved experiments. The capillary of 0.7 mm containing the sample was rotated during data collection to improve diffracting particle statistics. The data acquisition time was 10 min per pattern, and the final

treated data are the addition of 10 acquisitions to attain a very good signal-tonoise ratio over the angular range 0.5−43.6° (2θ) at 100 K.

2.2.2. Single Crystal X-ray Diffraction. Ago-AA Form II. MAR345 diffractometer with an image plate detector was used. Intensity data were collected with graphite monochromatized MoKα radiation (λ = 0.71073 Å) using a ϕ-scan technique. The structures were solved by direct methods, using the SHELXS computer program, and refined by full-matrix least-squares method with the SHELX97 computer program. Ago-HQ Form I, Ago-OA Form I and Ago-PA. A D8 Venture system equipped with a Multilayer monochromator and a Mo microfocus (λ = 1.54178 Å) was used. The structures were solved using the Bruker SHELXTL Software Package and refined using SHELXL.11

2.2.3. Differential Scanning Calorimetry (DSC). Differential scanning calorimetry was carried out by means of a Mettler-Toledo DSC-822e calorimeter. Experimental conditions: aluminum crucibles of 40 μL volume, atmosphere of dry nitrogen with 50 mL/min flow rate, and heating rate of 10 °C/min. The calorimeter was calibrated with indium of 99.99% purity. All the melting points reported have been measured under these conditions.

2.2.4. Thermogravimetric Analysis (TGA). Thermogravimetric analyses were performed with all solids obtained during the screening to detect the presence of solvates on a Mettler-Toledo TGA-851e thermobalance. Experimental conditions: alumina crucibles of 70 μL volume, atmosphere of dry nitrogen with 50 mL/min flow rate, and heating rate of 10 °C/min.

2.2.5. Miller. Liquid-assisted grinding experiments were performed with a Retsch ball mill MM 2000 equipped with two metal vessels, each with four 2 mL cavities. Two tungsten balls (diameter 3 mm) were used in each experiment which was performed at 30 Hz for 15 or 30 min.

3. RESULTS AND DISCUSSION

3.1. Bibliographic Search. Recently, a search of polymorphic cocrystals that contain at least two neutral organic solid components under ambient conditions has been reported showing 110 systems.5 We have updated this information by analyzing the Cambridge Structural Database (CSD, November 2014), and we have found 128 polymorphic cocrystals (Refcodes included in Supporting Information (SI)), involving 165 different compounds. Among them, 41 compounds (a list can be found in SI) appear in more than one system. These data suggest that it is quite likely from a statistical point of view that compounds forming polymorphic cocrystals with one coformer will do the same with other coformers. This tendency is observed in the case of agomelatine as we report in the present study two polymorphic cocrystals with acetic acid and hydroquinone.

3.2. Cocrystal Screening. Agomelatine contains a secondary amide group which can be involved in supramolecular heterosynthons with different complementary functional groups such as carboxylic acids, alcohols, esters, amides, etc. as it has been demonstrated by the cocrystals previously reported.9,10 Therefore, based on this information, we have investigated a number of coformers (see SI). After performing drop grinding experiments with equimolar amounts of agomelatine and each coformer, the previously described cocrystals in the literature were detected together with new cocrystals with hydroquinone, acetic acid, pyruvic acid, and oxalic acid.

Results of liquid-assisted grinding experiments between agomelatine and hydroquinone and oxalic acid with one drop of four different solvents (water, acetonitrile, ethyl acetate, and cyclohexane) are shown in Table 1. As it can be seen, two different cocrystals for each coformer were obtained depending on the solvent used in liquid-assisted grinding experiments. It has been previously reported that liquid-assisted grinding methodology can provide a successful means of controlling the polymorphic outcome of cocrystallization. For example, in the case of caffeine and glutaric acid, the addition of some drops of a nonpolar solvent (such as n-hexane, cyclohexane, or heptane) to equimolar quantities of caffeine and glutaric acid resulted in cocrystal form I. Conversely, the addition of some drops of a more polar solvent, including chloroform, dichloromethane, acetonitrile, and water, yielded cocrystal form II with identical secondary architecture.12 A similar observation has been reported for the polymorphic cocrystals of caffeine and anthranilic acid (both polymorphs exhibit the same synthon) where the dipole moment and the functional group of the solvent seemed to play a role, and only if the solvent molecule had a high dipole moment, was cocrystal form II formed, nitromethane being an exception despite its high dipole moment.13 Another example shows a high degree of solvent polarity specificity for the grinding experiments between 5-fluorouracil and 4-hydroxybenzoic acid.14 In the case of the new agomelatine cocrystals the solvent also plays a major role in the solid form outcome of grinding experiments with hydroquinone, but it is rather irrelevant with oxalic acid. However, a correlation between the polarity of the solvent and the solid form obtained is not clear, showing that the cocrystallization kinetic landscape of a compound can be a very complex issue influenced by many factors. Regarding the oxalic acid cocrystals, Form II of the Ago-OA cocrystal was always obtained as a mixture with Form I, and attempts to obtain it by using other methodologies such as slurries or crystallizations were unsuccessful, so it has not been further studied.

The relative stability between both polymorphs of the hydroquinone cocrystal has been determined. Suspensions of an equimolar mixture of Ago-HQ Form I and Form II in diisopropylether or toluene transformed into pure Form II after 3 days, showing that Form I is metastable at room temperature. Moreover, DSC analysis of Form I shows its melting at 81 °C with simultaneous crystallization of Form II which melts at 93 °C, suggesting that both polymorphs are monotropically related since the highest melting form is the most stable one at room temperature (Figure 2).16

Regarding acetic acid and pyruvic acid coformers, which unlike hydroquinone and oxalic acid are liquids at room temperature, grinding experiments between agomelatine and one drop of each coformer were performed. A new acetic acid cocrystal different from the previously reported9 and a mixture of Agomelatine Form II and pyruvic acid cocrystal were obtained, respectively. Both cocrystals were also obtained by slow crystallization from a solution of agomelatine in either acetic acid or pyruvic acid.

3.3. Crystal Structures Analysis. 3.3.1. Hydroquinone Polymorphic Cocrystals. Two polymorphs of the hydroquinone cocrystal with 1:1 stoichiometry were obtained. Form I was solved by single crystal XRD. However, attempts to grow quality crystals of Form II were unsuccessful. Thus, the resolution of its crystal structure was achieved by using the direct space methodology.

The structure has been determined using synchrotron X-ray powder diffraction data obtained in the high-resolution powder diffraction end station of the MSPD beamline in Alba. The right data have been obtained with the sample in a 0.7 glass capillary, at 100 K, with a wavelength of 0.6194 Å using the Mythen detector. Attempts to index high resolution powder diffraction data with Cu Kα laboratory X-ray powder diffraction data at room temperature has not been successful. The 100 K synchrotron powder diffraction data was perfectly indexed to an orthorhombic cell of about 1830 Å3 by means of Dicvol04,17 and the space group was perfectly determined to be P212121 from the systematic absences. The asymmetric unit being one molecule (1:1 agomelatine/hydroquinone stoichiometry), Z = 4, the crystal structure was determined by direct space methodologies starting from a molecular model optimized with the commercial software SPARTAN by means of the program FOX18 with the parallel tempering algorithm. Some constraints were introduced to FOX, considering aromatic rings as rigid groups. Several trials of 20 million runs were performed. The refinement of the structure has been performed by the Rietveld method using FullProf.19 Rwp = 3.54%, Chi2 = 80 (compared to Le Bail fit: Rwp = 2.24%, Chi2 = 32) Figure 3 depicts the final Rietveld plot.

Synthon polymorphism occurs when the primary synthons in the forms are different20 as it is the present case of the two polymorphs of the agomelatine−hydroquinone cocrystal.

In Form I, hydroquinone molecules form chains in a cis conformation, with the hydroxyl groups of each molecule acting simultaneously as H-bond acceptor and donor. Layers of agomelatine molecules are intercalated between the hydroquinone chains stabilized through H-bonds involving both CO and NH groups of each molecule of agomelatine.

On the other hand, in Form II only the carbonylic oxygen of each agomelatine is involved in a hydrogen bond with hydroquinone (Figure 4).

Interestingly, the agomelatine molecules do not interact with other agomelatine molecules in the usual amide/amide selfassembling motif observed in the three agomelatine polymorphs (Refcodes: WERNOW,8 WERNOW01,9 and WERNOW029). In Form II, again hydroquinone molecules adopt the cis conformation forming similar self-assembling chains as in Form I, but the most relevant difference with respect to Form I is that a NH···π interaction is established between the agomelatine amidic proton and the hydroquinone aromatic ring (NH···centroid distance of 2.58 Å). Moreover, the naphthalene moieties of agomelatine establish two CH···π interactions (CH···centroid distances of 2.53 and 2.83 Å), Figure 5.

The hydrogen bonding interaction between the amide group and the aromatic ring is less frequent in crystal structure of proteins, where the amide/amide is much more predominant, the NH···π interaction in proteins being first reported by Perutz in 1986.21 However, ab initio calculations revealed that the NH···π interaction, although weaker than a conventional hydrogen bond, is still significant (up to 3.5 kcal/mol,22 so as Hunter suggested “H-bonding to the face of aromatic rings may play a significant role in molecular recognition phenomena in different environments”),23 as it has been demonstrated in Form

II, where the strong amide/amide interaction is not observed, while CH···π and NH···π interactions are relevant.

Another remarkable difference between both polymorphs is the different orientation of the self-assembled hydroquinone chains. While in Form I chains are almost perpendicular, in Form II they are parallel (Figure 6). Moreover, while in the chains of Form II the hydroquinone molecules are coplanar, in those of Form I hydroquinone molecules show some displacement from coplanarity. Interestingly, in both polymorphs, the hydroquinone molecules adopt the cis configuration, which is unusual according to the reported search in the CSD in which the 87.5% of the 137 analyzed containing hydroquinone structures were in the trans configuration.24 The absence of inversion centers in both crystal structures can explain the cis configuration observed in the hydroquinone molecule of both polymorphs and give additional support to the hypothesis by Pidcock et al.25 in the sense that the molecules with inversion centers tend to preserve it mainly in centrosymmetric crystal structures.

3.3.2. Pyruvic Acid Cocrystal. The pyruvic acid cocrystal was also solved by single crystal XRD. The structure of the pyruvic acid cocrystal shows a hydrogen-bond interaction pattern following the expected hierarchical order between the best donor and the best acceptor of both agomelatine and pyruvic acid, forming ribbons with an alternate amide/acid supramolecular synthon. Moreover, the pyruvic acid cis conformation allows the two carbonylic oxygens to point toward the NH proton in an equidistant way (NH···OC distance of 2.32 Å) (Figure 7).

Interestingly, the crystal structure can be described as hydrogen-bonded aggregates of self-assembled units formed by two agomelatine and two pyruvic acid molecules. The most remarkable issue of these units is that they are kept together by the combination of two different kind of interactions: classical amide/carboxylic acid hydrogen bond together with the less frequent π···π interaction between the naphthalene rings and the carbonyl groups of pyruvic acid. It has been previously demonstrated through ab initio quantum mechanical calculations26 that parallel C⊕O/aromatic ring interactions are favorable with centroid-oxygen distances of around 3.0−3.5 Å. Although in the pyruvic acid cocrystal these distances are slightly longer (3.58 and 3.67 Å, Figure 8) the almost perfect parallel stacking confirms this aromatic interaction observed, to some extent, in the crystal structure of proteins.

3.3.3. Acetic Acid Polymorphic Cocrystals. A new polymorph of the acetic acid cocrystal with 1:1 stoichiometry has been obtained. Form I had been previously described in the literature,9 and Form II was solved by single crystal XRD. Both polymorphs show the same hydrogen-bond interactions following the expected hierarchical order between the best donor and the best acceptor of both agomelatine and acetic acid. However, while in Form I the amide and carboxylic acid groups form right-hand cooperative helices through the alternation of NH···O and OH···O hydrogen bonds, in Form II the same interaction is topologically structured in ribbons (Figure 9). Helixes of Form I are interconnected through CH···π interactions (CH···centroid distance of 2.97 Å) in an alternated zigzag arrangement of agomelatine molecules, while layers in Form II are connected through CH···π interactions (CH···centroid distance of 2.68 Å) between the acetic acid methyl group and the aromatic face of agomelatine (Figure 10).

Moreover, in Form II the parallel C⊕O/aromatic ring interaction is also observed with a centroid−oxygen distance of 3.56 Å.

3.3.4. Oxalic Acid Cocrystals. A new oxalic acid cocrystal has been identified during the screening. Its crystal structure solved by means of single crystal XRD shows a 2:1 stoichiometry. The analysis of the structure reveals that oxalic acid displays a conformation with both carboxylic groups in a perpendicular fashion with a 2-fold axis passing through the center of the molecule, which enables four molecules of

agomelatine to surround it, resembling a calix and establishing strong hydrogen-bonding interactions (Figure 11).

This supramolecular aggregate is repeated thanks to the dual donor/acceptor ability of the amide group, which forms ribbons of alternate acid/amide interacting groups (Figure 12). Again and in a similar way as in the cocrystal with hydroquinone, the naphthalene moieties of agomelatine establish two longer CH···π interactions (CH···centroid distances of 2.89 and 3.24 Å).

3.3.5. Hydrogen Bonding Synthons of Agomelatine Cocrystals. Yan et al.10 in their paper about agomelatine cocrystals in 2012 presented a scheme showing the possible hydrogen bonding synthons involving the secondary amide group of this API with different functional groups such as amide, carboxylic acid, alcohol, and ester of possible coformers. As a summary, we have analyzed the synthons exhibited in each of the 11 cocrystals of agomelatine (Figure 13).

Coformers with carboxylic acid as a unique functional group (acetic acid and oxalic acid) as well as pyruvic acid (which contains an additional carbonyl group) exhibit synthons II and III. Synthon I occurs in urea and isonicotinamide cocrystals as expected for coformers with amide functional groups. Cocrystals with ethylene glycol and hydroquinone, which contain alcohols, exhibit synthons V and VI. However, a new synthon NH···π between the amide and the aromatic group (synthon VII) is observed in Ago-HQ Form II, instead of synthon VI. Moreover, coformers with two different functional groups such as glycolic acid (carboxylic acid and alcohol) and methyl-4-hydroxybenzoate (ester and phenol) exhibit synthons involving both functional groups. In the case of glycolic acid, synthons III and VI are formed, whereas for methyl-4- hydroxybenzoate, synthons IV and V are observed. Cocrystals are ideally suited to study competition between different supramolecular heterosynthons. In both cocrystals, synthons are formed between the best H-bond acceptor (alcohol vs carboxylic acid and ester vs phenol) and the best H-bond donor (carboxylic acid vs alcohol) as expected according to Hunter's hydrogen bonding parameters.27,28

4. CONCLUSIONS

The present study is focused on extending the knowledge about the multicomponent forms of the drug compound agomelatine. New cocrystals with hydroquinone and several carboxylic acids have been discovered through an intensive cocrystal screening, and their crystal structures were solved by means of direct space methods together with single crystal X-ray diffraction data. Our results reveal the existence of polymorphism at least in two of the new cocrystals showing important differences regarding the type of intermolecular interactions involved in the crystal, which convert agomelatine in another case to enrich the list of compounds showing cocrystal polymorphism and at the same time contribute to dismantle the belief that cocrystals are less prone to exhibit polymorphism than single component crystals.

AUTHOR INFORMATION

Corresponding Authors

*(R.P.) Tel. + 34 93 4034656. Fax. + 34 93 4037206. E-mail: rafel@ccit.ub.edu.

*(C.P.) E-mail: cris@ccit.ub.edu.

REFERENCES

(1) Cruz-Cabeza, A. J.; Reutzel-Edens, S. M.; Bernstein, J. Chem. Soc. Rev. 2015, 44, 8619−8635.

(2) Stahly, G. P. Cryst. Growth Des. 2007, 7, 1007−1026.

(3) Butterhof, C.; Bärwinkel, K.; Senker, J.; Breu, J. CrystEngComm 2012, 14, 6744−6749.

(4) Clarke, H. D.; Arora, K. K.; Bass, H.; Kavuru, P.; Ong, T. T.; Pujari, T.; Wojtas, L.; Zaworotko, M. J. Cryst. Growth Des. 2010, 10, 2152−2167.

(5) Aitipamula, S.; Chow, P. S.; Tan, R. B. H. CrystEngComm 2014, 16, 3451−3465.

(6) Lemmerer, A.; Adsmond, D. A.; Esterhuysen, C.; Bernstein, J. Cryst. Growth Des. 2013, 13, 3935−3952.

(7) Taylor, D.; Sparshatt, A.; Varma, S.; Olofinjana, O. BMJ 2014, 348, g1888.

(8) Tinant, B.; Declercq, J.-P.; Poupaert, J. H.; Yous, S.; Lesieur, D. Acta Crystallogr., Sect. C: C ryst. Struct. Commun. 1994, 50, 907−910.

(9) Zheng, S.-L.; Chen, J.-M.; Zhang, W.-X.; Lu, T.-B. Cryst. Growth Des. 2011, 11, 466−471.

(10) Yan, Y.; Chen, J.-M.; Geng, N.; Lu, T.-B. Cryst. Growth Des. 2012, 12, 2226−2233.

(11) Sheldrick, G. M. Acta Crystallogr., Sect. A: Found. Crystallogr. 2008, 64, 112−122.

(12) Trask, A. V.; Motherwell, W. D. S.; Jones, W. Chem. Commun. 2004, 890−891.

(13) Fischer, F.; Scholz, G.; Benemann, S.; Rademann, K.; Emmerling, F. CrystEngComm 2014, 16, 8272−8278.

(14) Li, S.; Chen, J.-M.; Lu, T.-B. CrystEngComm 2014, 16, 6450−6458.

(15) Solvent property parameters: Gu, C.-H.; Li, H.; Gandhi, R. B.; Raghavan, K. Int. J. Pharm. 2004, 283, 117−125.

(16) Barbas, R.; Prohens, R.; Puigjaner, C. J. Therm. Anal. Calorim. 2007, 89, 687−692.

(17) Boultif, A.; Louer, D. J. Appl. Crystallogr. 1991, 24, 987.

(18) Favre-Nicolin, V.; Cerny, R. J. Appl. Crystallogr. 2002, 35, 734−743.

(19) Rodriguez-Carvajal, J. Phys. B 1993, 192, 55−69.

(20) Jetti, R. K. R.; Boese, R.; Sarma, J. A. R. P.; Reddy, L. S.;Vishweshwar, P.; Desiraju, G. R. Angew. Chem., Int. Ed. 2003, 42, 1963−1967.

(21) Perutz, M. F.; Fermi, G.; Abraham, D. J.; Poyart, C.; Bursaux, E. J. Am. Chem. Soc. 1986, 108, 1064−1078.

(22) Steiner, T.; Koellner, G. J. Mol. Biol. 2001, 305, 535−557.

(23) Adams, H.; Carver, F. J.; Hunter, C. A.; Osborne, N. J. Chem. Commun. 1996, 2529−2530.

(24) Clausen, H. F.; Chevallier, M. S.; Spackman, M. A.; Iversen, B.B. New J. Chem. 2010, 34, 193−199.

(25) Pidcock, E.; Motherwell, W. D. S.; Cole, J. C. Acta Crystallogr., Sect. B: Struct. Sci. 2003, 59, 634−640.

(26) Jain, A.; Purohit, C. S.; Verma, S.; Sankararamakrishnan, R. J.Phys. Chem. B 2007, 111, 8680−8683.

(27) Etter, M. C. Acc. Chem. Res. 1990, 23, 120−126.

(28) Hunter, C. A. Angew. Chem., Int. Ed. 2004, 43, 5310−5324.

.

Legends to figures

Figure 1. Chemical structure of agomelatine.

Figure 2. DSC of agomelatine−hydroquinone cocrystals.

Figure 3. Results from powder XRD analysis of Form II of hydroquinone/agomelatine cocrystal: (left) Final Rietveld plot for the crystal structure refinement. Agreement factors: Rwp = 3.54%, Rp = 2.51%, (right) Le Bail fit plot. Agreement factors: Rwp = 2.24%, Rp = 1.46%. Each plot shows the experimental powder XRD profile (red + marks), the calculated powder XRD profile (black solid line), and the difference profile (blue, lower line). Tick marks indicate peak positions.

Figure 4. Amide/phenol hydrogen-bond interactions between agomelatine and hydroquinone in Form I (a) and Form II (b).

Figure 5. (a) NH···π interaction between the amide and the electron density on the face of the hydroquinone ring in Form II and (b) CH···π interactions between the naphthalene moieties in Form II.

Figure 6. Different arrangement of hydroquinone ribbons in Form II (a) and Form I (b).

Figure 7. Ribbon arrangement of agomelatine pyruvic acid cocrystal. Agomelatine structure has been truncated.

Figure 8. Self-assembled units of agomelatine and pyruvic acid.

Figure 9. Helicoidal topology of Form I (a) and ribbon arrangement of Form II (b) of acetic acid cocrystals.

Figure 10. CH···π interactions in Form I (a) and in Form II (b) of acetic acid cocrystals.

Figure 11. Molecules of agomelatine surrounding oxalic acid in the 2:1 cocrystal. Agomelatine methoxy groups have been omitted for clarity.

Figure 12. Ribbon arrangement of agomelatine oxalic acid cocrystal.

Figure 13. Hydrogen bonding synthons present in agomelatine cocrystals.

411 **FIGURE 1.**

412

413

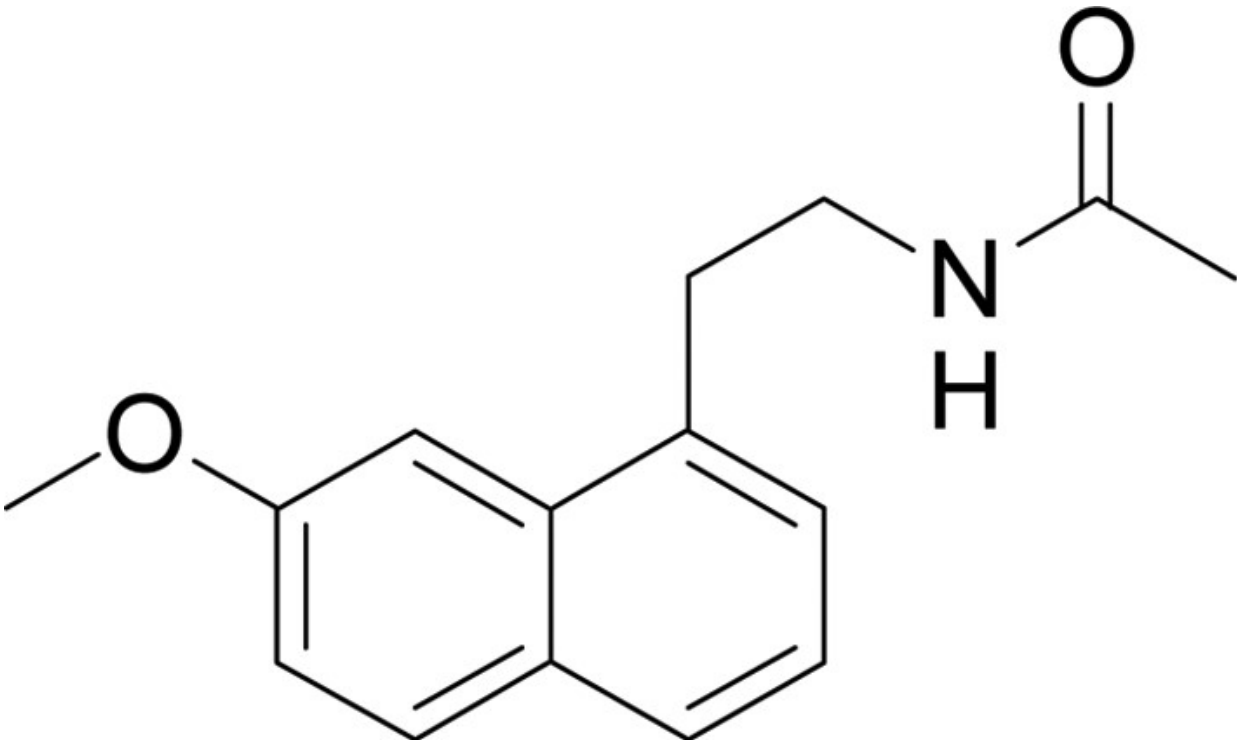

414

415

FIGURE 2.

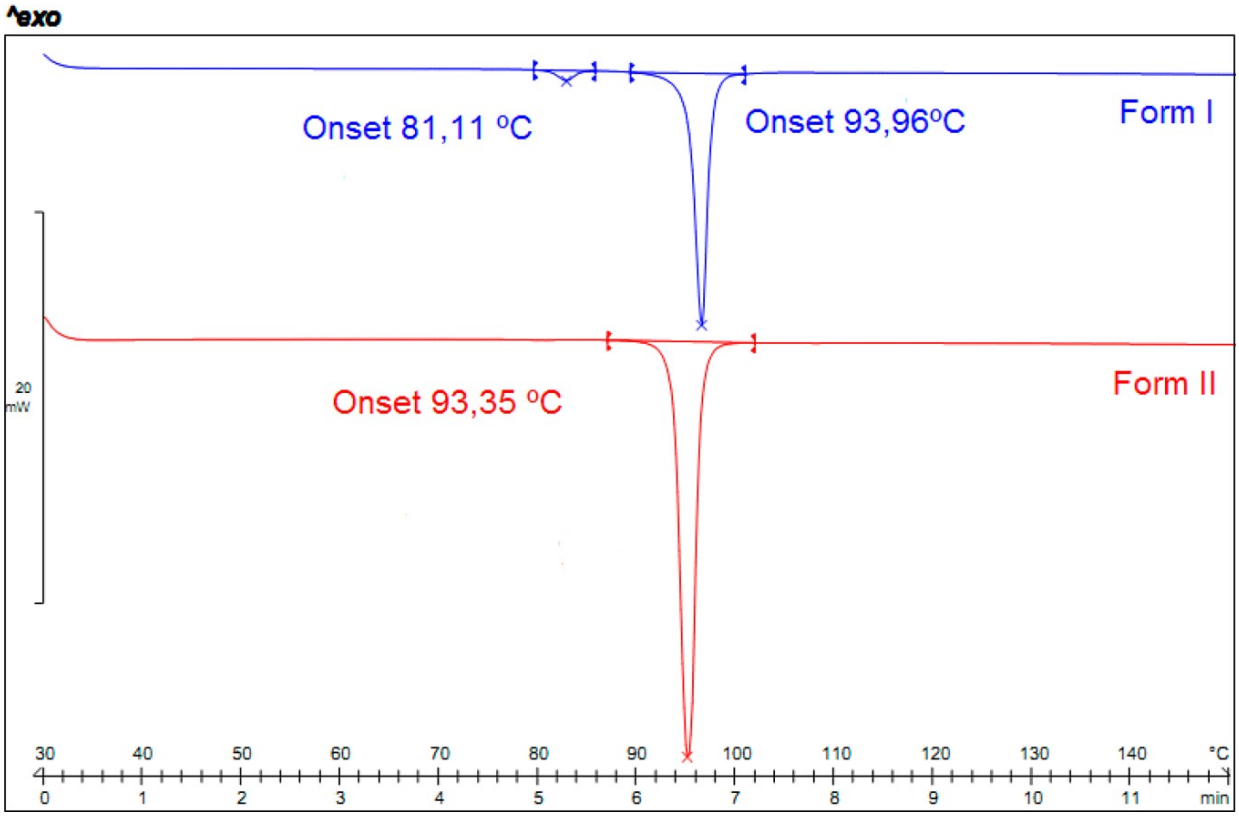
exo
Onset 81,11 °C
Onset 93,96°C
Form I
20
mW
Onset 93,35 °C
Form II
30 40 50 60 70 80 90 100 110 120 130 140 °C
0 1 2 3 4 5 6 7 8 9 10 11 min

422 **FIGURE 3.**

423

424

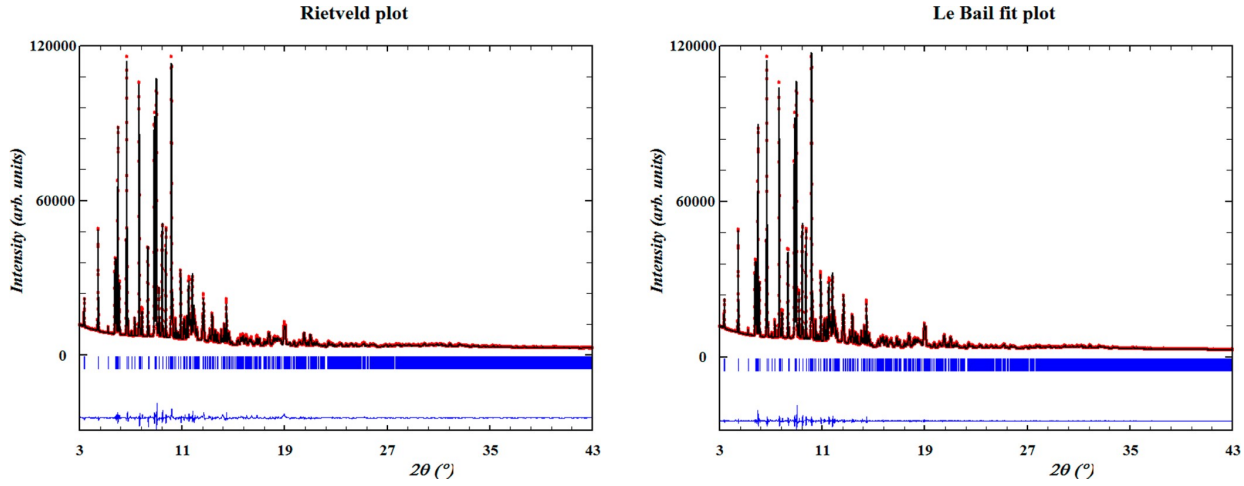

425

426

FIGURE 4.

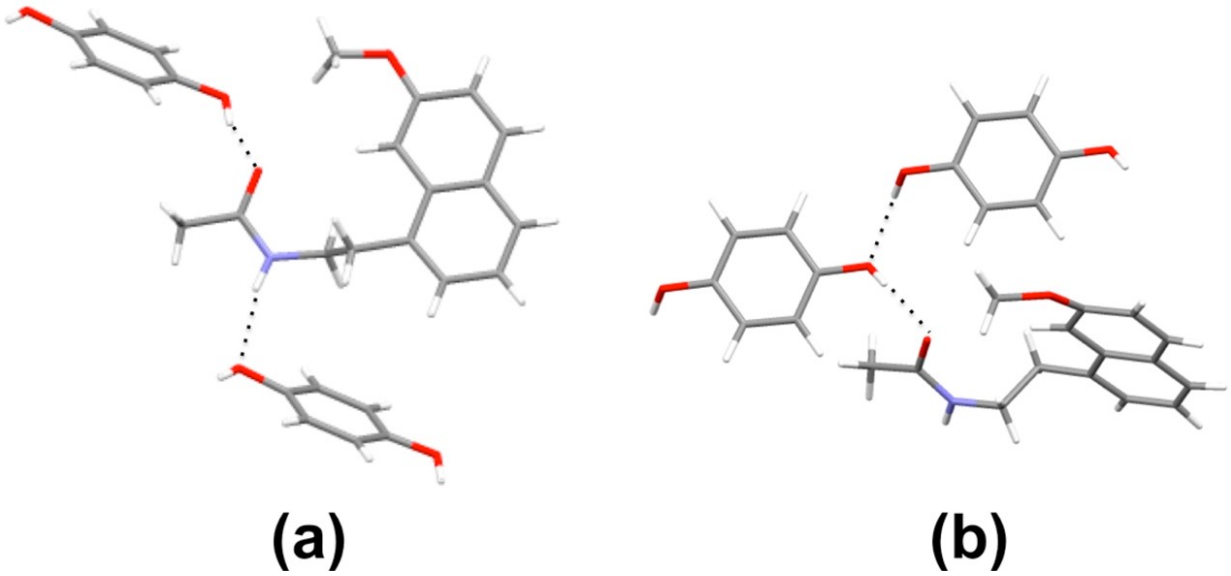

FIGURE 5.

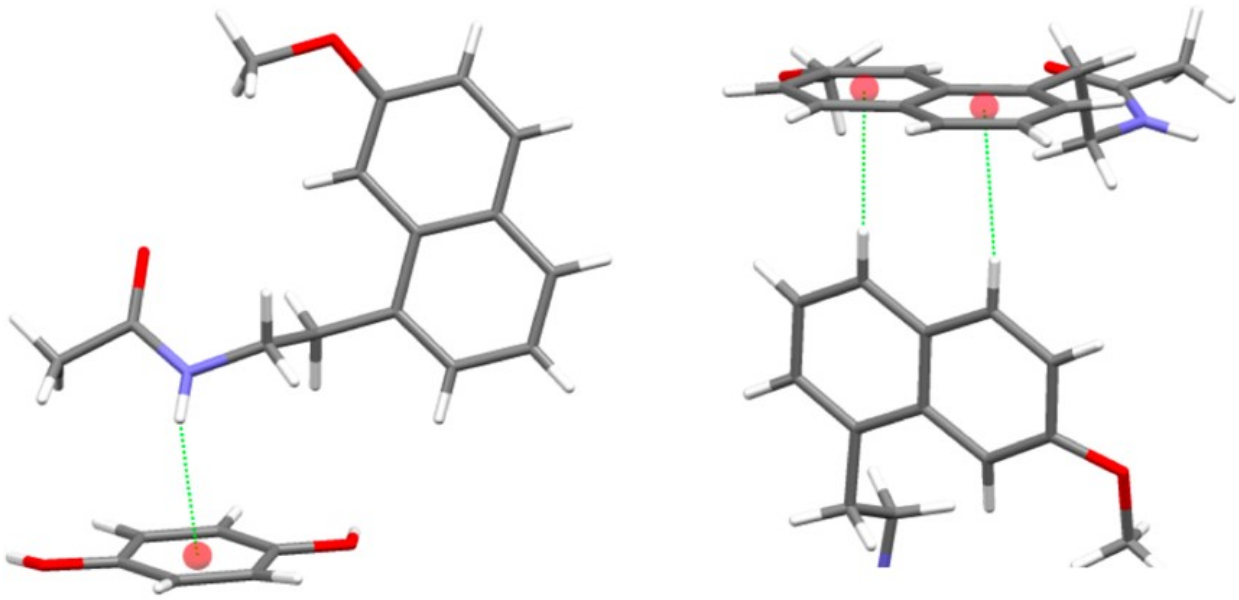

FIGURE 6.

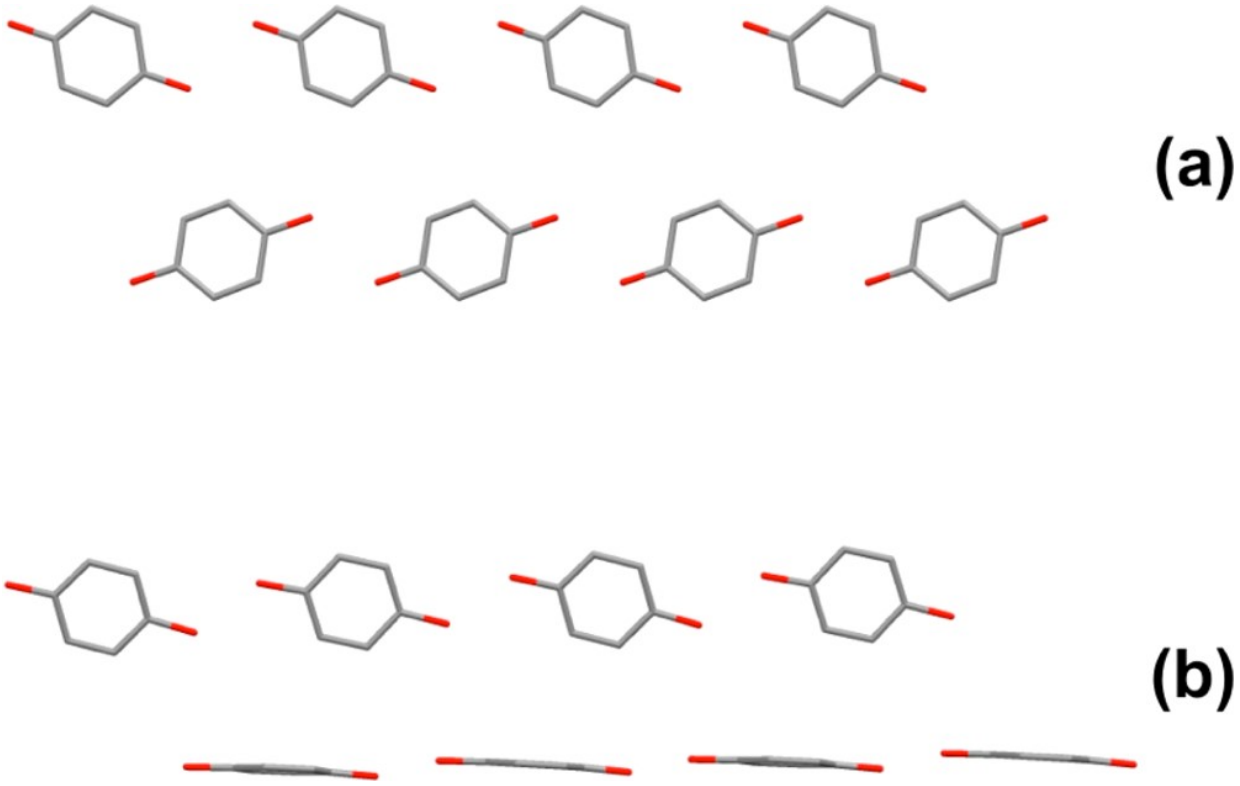

FIGURE 7.

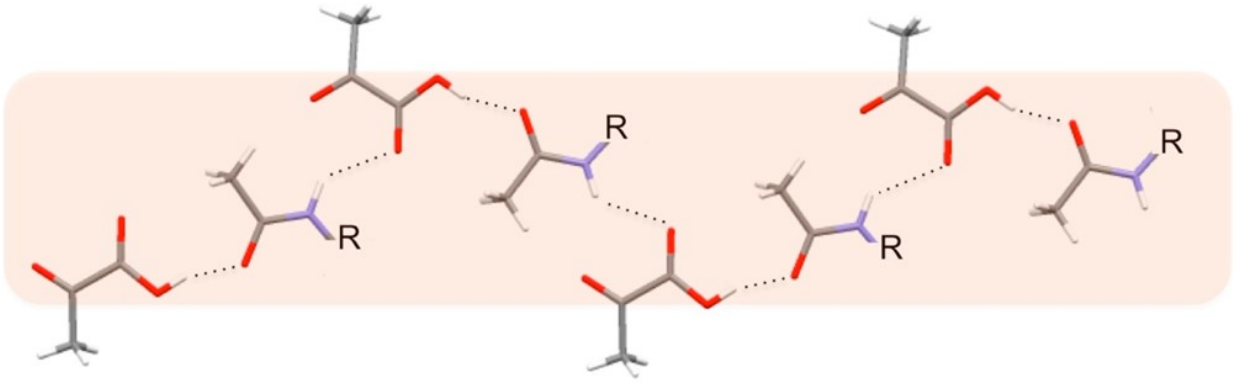

FIGURE 8.

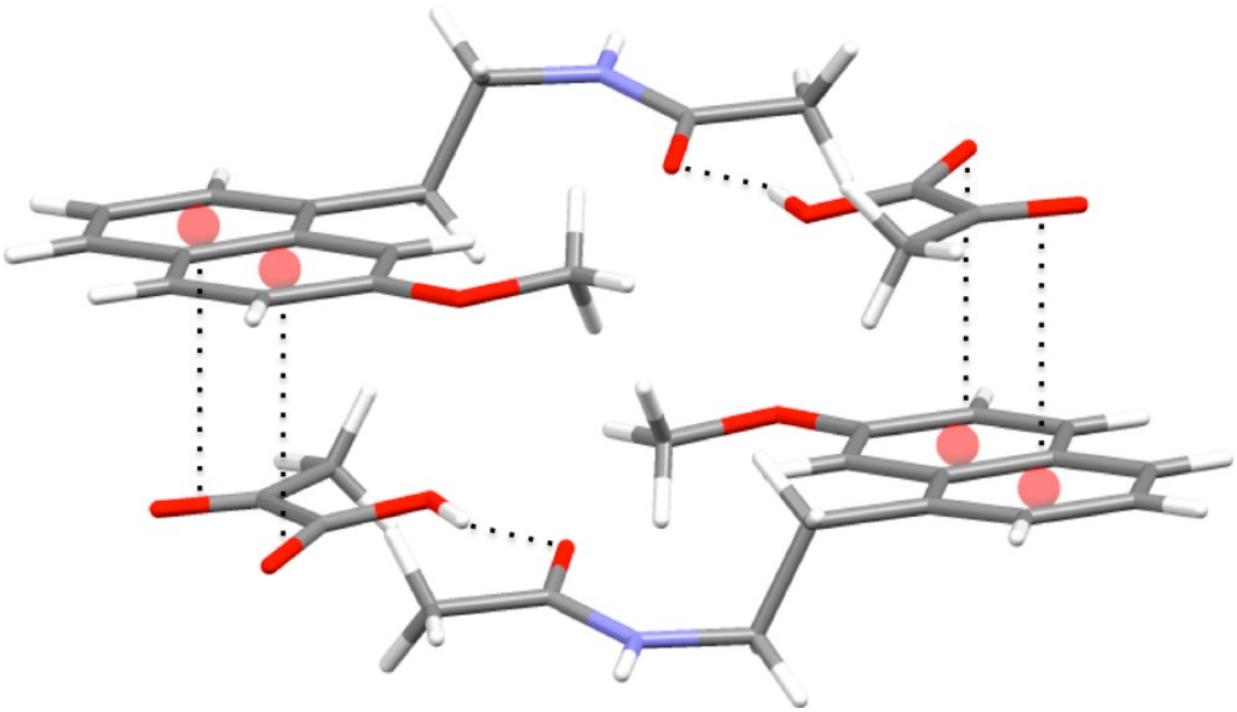

FIGURE 9.

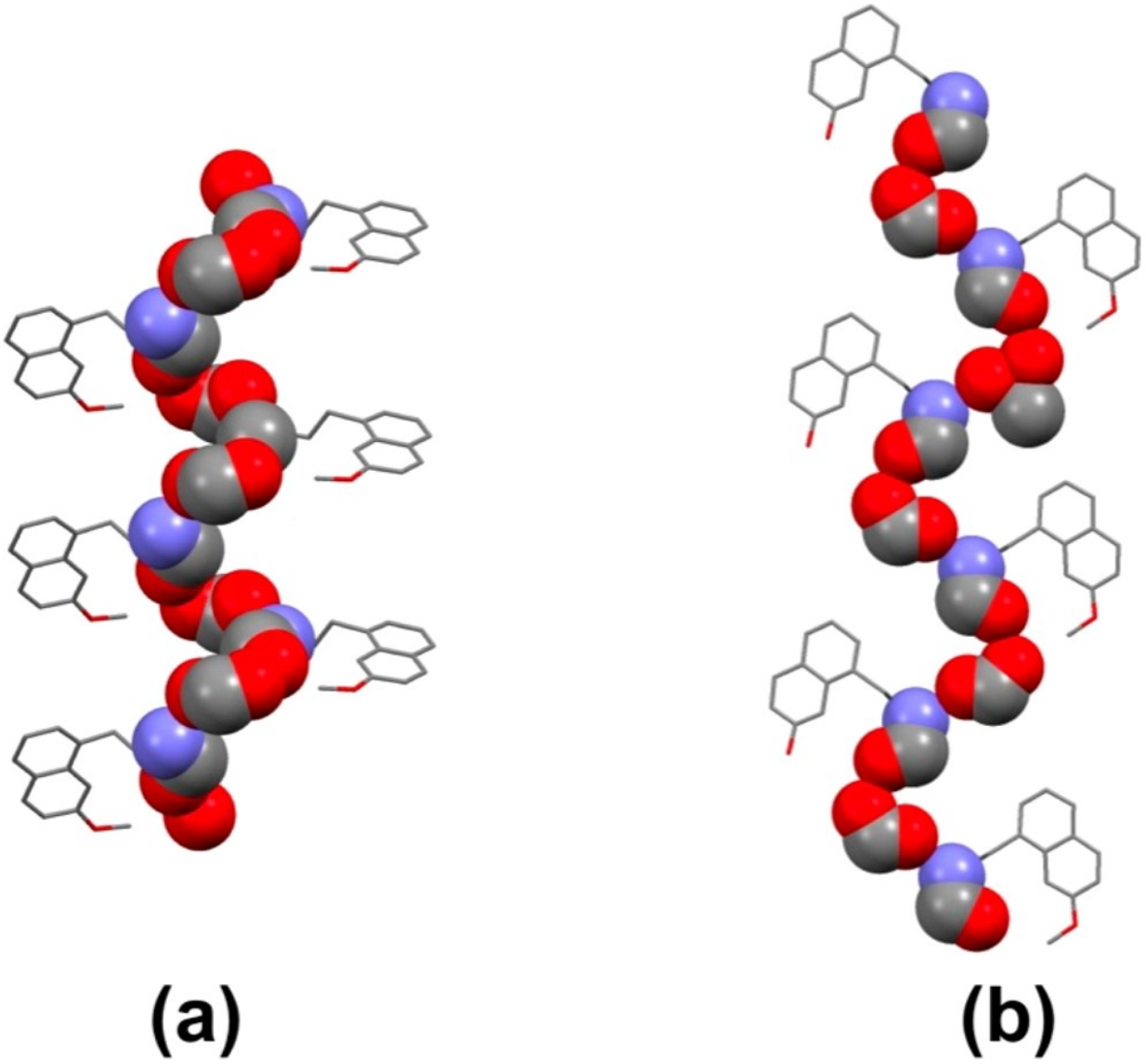

458 **FIGURE 10.**

459
460

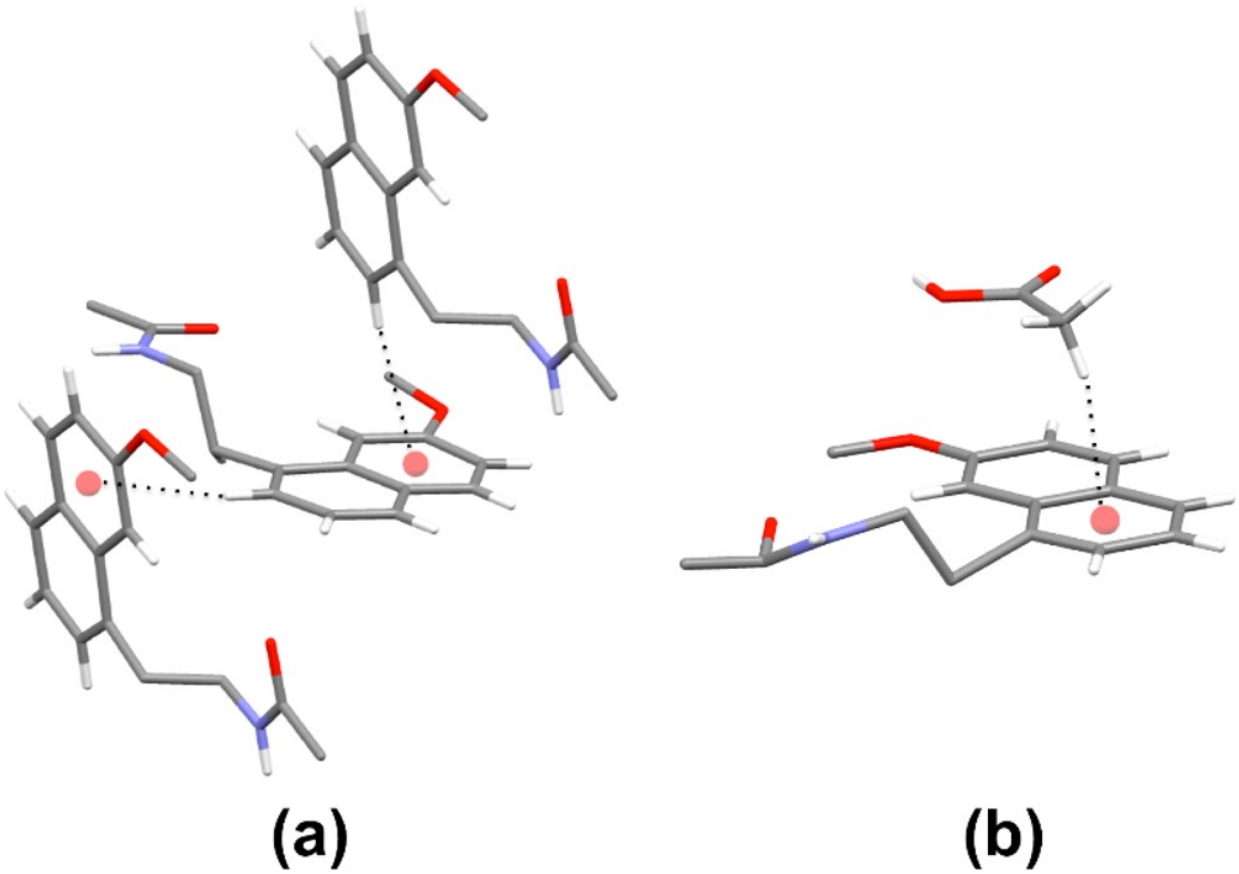

461
462
463

FIGURE 11.

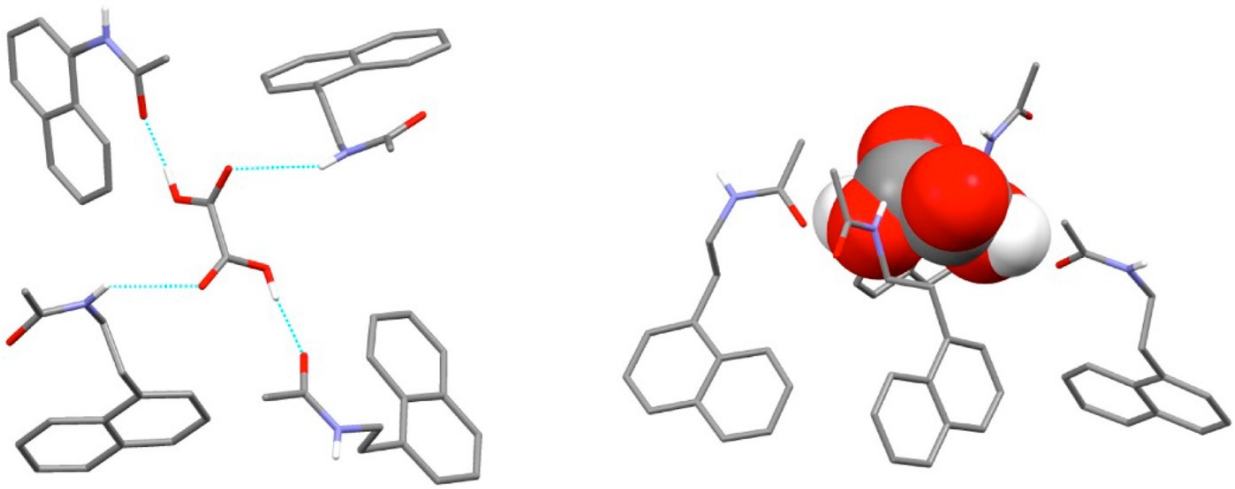

FIGURE 12.

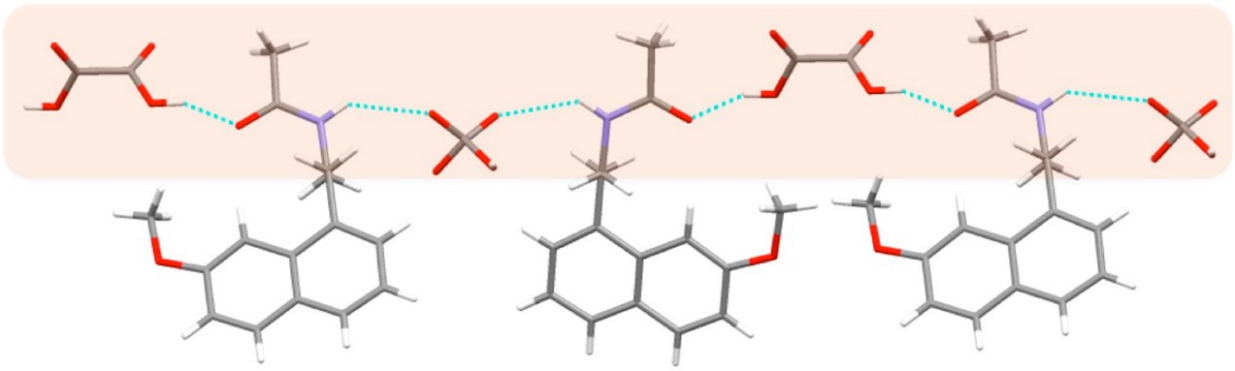

476 **FIGURE 13.**

477
478

Amide

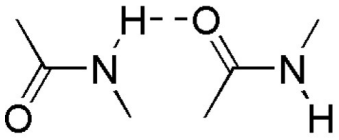

I

Carboxylic Acid

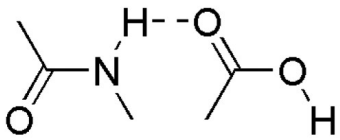

II

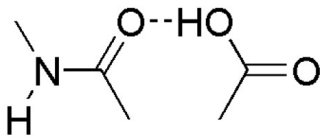

III

Ester

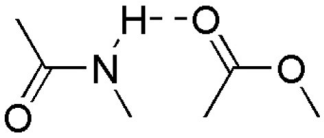

IV

Alcohol

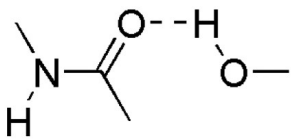

V

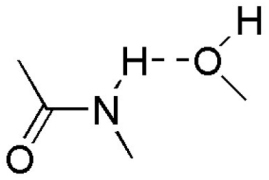

VI

Aromatic

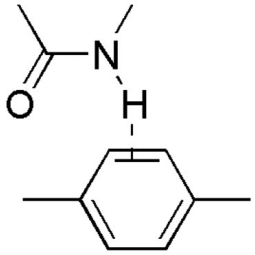

VII

479
480
481

482 **Table 1** Liquid-Assisted Grinding Experiments15 a
483

Table 1. Liquid-Assisted Grinding Experiments[15,a]

solvent	ε	π	results with hydroquinone	results with oxalic acid
water	78.36	1.09	Ago-HQ Form I	Ago-OA Form I + Ago-OA Form II[b]
acetonitrile	35.69	0.75	Ago-HQ Form II	Ago-OA Form I[b]
ethyl acetate	5.99	0.55	Ago-HQ Form II	Ago-OA Form I[b]
cyclohexane	2.02	0.00	Ago-HQ Form I	Ago-OA Form I[b]

[a] ε: dielectric constant; π: polarity. [b] Oxalic acid was also obtained together with Ago-OA cocrystals.

484
485
486
487
488
489

Table 2. Crystal Data and Structure Refinement Parameters for the Different Forms of Agomelatine Cocrystals

structure	Ago-HQ Form I	Ago-HQ Form II	Ago-AA Form II	Ago-OA	Ago-PA
empirical formula	$C_{15}H_{17}NO_2$, $C_6H_6O_2$	$C_{15}H_{17}NO_2$, $C_6H_6O_2$	$C_{17}H_{21}NO_4$	$2(C_{15}H_{17}NO_2)$, $C_2H_2O_4$	$C_{18}H_{21}NO_5$
formula weight	353.40	353.40	303.35	576.68	331.36
temperature (K)	106(2)	100	293(2)	302	90(2)
wavelength (Å)	0.71073	0.6196	0.71073	1.54178	0.71073
crystal system	monoclinic	orthorhombic	orthorhombic	monoclinic	monoclinic
space group	$P2_1$	$P2_12_12_1$	*Pnma*	C2	C2/c
a, b, c (Å)	10.8611(15) 28.563(4) 12.0118(17)	21.202.50(14) 12.04722(7) 7.15198(5)	14.224(7) 7.062(3) 16.348(5)	27.8783(17) 7.5821(6)19.7562(14)	18.2641(13), 15.5402(11), 14.6089(17)
α, β, γ (deg)	90, 100.318(5), 90	90°, 90°, 90°	90°, 90°, 90°	90, 133.745(4), 90	90, 126.779(2), 90
volume (Å^3)	3666.1(9)	1826.84(2)	1641.9(12)	3016.8(4)	3319.9(5)
Z, density (calc) (Mg/m^3)	8, 1.281	4	4/1.227	4/1.270	8, 1.326
absorption coefficient (mm^{-1})	0.088		0.087	0.753	0.097
$F(000)$	1504		648	1224	1408
crystal size (mm^3)	0.583 × 0.468 × 0.431		0.2 × 0.1 × 0.1	0.16 × 0.13 × 0.09	0.14 × 0.12 × 0.09
θ range for data collection (deg)	2.237−26.371	2.00−43.58	1.898−30.815	3.10−58.89	2.62−25.10
limiting indices	$-13 \le h \le 13$		$-18 \le h \le 18$	$-30 \le h \le 30$	$-21 \le h \le 21$
	$-35 \le k \le 35$		$-8 \le k \le 8$	$-8 \le k \le 8$	$-18 \le k \le 18$
	$-15 \le l \le 15$		$-21 \le l \le 21$	$-21 \le l \le 21$	$-17 \le l \le 17$
reflections collected/unique	73951/14971 [R(int) = 0.0770]		11977/2208 [R(int) = 0.0638]	4774/2958 [R(int) = 0.0879]	20241/2947 [R(int) = 0.0444]
completeness to θ (%)	99.9		95.9	86.9	99.5
absorption correction	semiempirical from equivalents		empirical	semiempirical from equivalents	semiempirical from equivalents
max and min transmission	0.7459 and 0.6481		0.5 and 0.5	0.7516 and 0.5587	0.961 and 0.943
refinement method	full-matrix least-squares on F^2	Rietveld	full-matrix least-squares on F^2	full-matrix least-squares on F^2	full-matrix least-squares on F^2
data/parameters	14971/249/977	2406/87/131	2208/0/152	2958/8/380	2947/0/220
goodness-of - fit on F^2	1.009	Chi = 8.94	1.181	0.962	1.046
final R indices [$I > 2\sigma(I)$]	R_1 = 0.0410, wR_2 = 0.0890		R_1 = 0.0539, wR_2 = 0.1478	R_1 = 0.0641, wR_2 = 0.1015	R_1 = 0.0532, wR_2 = 0.1243
R indices (all data)	R_1 = 0.0616, wR_2 = 0.0988	Rwp = 3.54, Chi2 = 80	R_1 = 0.0675, wR_2 = 0.1585	R_1 = 0.1904, wR_2 = 0.1364	R_1 = 0.0716, wR_2 = 0.1417
largest diff. peak and hole (e·Å^{-3})	0.171 and −0.207		0.134 and −0.145	0.173 and −0.193	0.480 and −0.247
CCDC	1048038	1058734	1048035	1060576	1048039